Recent Res. Devel. in Soil Science, 1 (1997)

Centrifuge scaling of unstable infiltration

J.W. Griffioen[1], P.J. Culligan[2], D.A. Barry[3] and K. Banno[2]

[1]Civil Engineering Department, University of Western Australia, Nedlands, 6907, Western Australia; [2]Department of Civil and Environmental Engineering, Massachusetts Institute of Technology, Massachusetts, USA; and [3]Environmental Engineering Department, University of Western Australia, Nedlands, 6907, Western Australia

INTRODUCTION.

Unstable wetting fronts typically occur where the hydraulic conductivity increases in the direction of flow, e.g., infiltration into an initially dry soil comprising a fine grained material overlying a coarser material. As a result of imbalance between gravity and capillary forces, instabilities at the wetting front grow and propagate downward, producing a phenomenon known as fingers. Analytical expressions for finger spacing, size and velocity have been derived from linear stability analyses, and successfully applied to several laboratory experiments.

Centrifuge modelling is a novel way in which unstable wetting front behaviour can be modelled. During centrifuge modelling, an increase in the body force imposed upon the physical model is achieved by spinning a scaled-down version of a prototype at a constant rate. By maintaining appropriate scaling ratios, e.g., wetting fluid flux: hydraulic conductivity, a linear trend is expected between the acceleration level and the observed finger size.

The application of centrifugation in soil science is well established: Over 20 years ago, Alemi et al. (1) demonstrated the experimental determination of transport parameters in soil cores using centrifugal techniques. More recently, research work in the field of environmental engineering has made use of the method to investigate the behaviour of gravity-driven flow phenomena under realistic, but well controlled, boundary conditions (2, 3, 4, 5).

In this chapter we report a number of experiments which show that unstable fir_ er properties, including size, propagation rate and spacing, vary linearly with the induced acceleration. The collaborative experiments were conducted at the University of Western Australia, and Massachusetts Institute of Technology. Further, we outline some of the hydraulic properties that influence the phenomenon of unstable infiltration, and discuss how unstable wetting fronts are expected to perform under the increased body force introduced during centrifuge modelling.

CENTRIFUGE SCALING.

Geotechnical centrifuge modelling is an experimental method used to obtain soil stress conditions that are homologous in model and prototype (6). This is achieved by subjecting a scale soil model, where all linear dimensions are reduced by a factor N, to a centrifugal acceleration of N gravities, N*g* (
Figure 1). The 1*g* case is known as the prototype, while the scaled version is the model. At a constant rotational speed (ω = constant), the tangential acceleration is zero, while the centrifugal acceleration is $Ng = \omega^2 R$. N is also known as the scaling factor or acceleration level.

In addition to generating identical stress distributions, centrifuge modelling also accelerates the time scale for seepage processes as a result of the increased self weight of the permeant and the reduced length scale. Assuming that identical fluids and porous media are used in the centrifuge model, the seepage velocity is increased by a factor N, and the time for fluid flow to occur is reduced by a factor N^2.

Scaling relationships for flow phenomena in the centrifuge have been presented by various authors (7, 8, 9). For a reduced-scale centrifuge model test conducted using prototype soil and liquids, the relationships given in Table 1 are either self-evident or well established.

Arulanandan et al. (7) present eight dimensionless groups that can be derived by dimensional analysis from the parameters affecting solute transport under conditions of increased acceleration. The two groups applicable to unstable wetting are (10): Reynolds number, to measure the relative effects of density to viscosity, and the Capillary number, which is the ratio of capillary tension to surface tension.

Reynolds number, $Re = \rho v d/\mu$, (see Notation List for symbol definitions) must be kept below a threshold value ($Re < 1$) to ensure validity of Darcy's law (11). It is not essential that the Reynold's number is the same in model as prototype, only that $Re < 1$ in both. On the basis of theoretical analysis, Bear and Verruijt (11) suggest that the best assumption for the microscopic length, d, is $(k/n)^{1/2}$. Thus, for a sand with an average particle size of 0.06 cm, porosity, n, ~ 0.4 and permeability, $k \sim 10^{-7}$ cm^2, using water as the interstitial fluid ($\rho = 0.998$ g/cm^3, $\mu = 10^{-2}$ g/cm/s), the critical velocity is approximately 460 cm/min. Since the critical velocity is more than twice the fastest velocity reported here, the Reynolds number condition is satisfied.

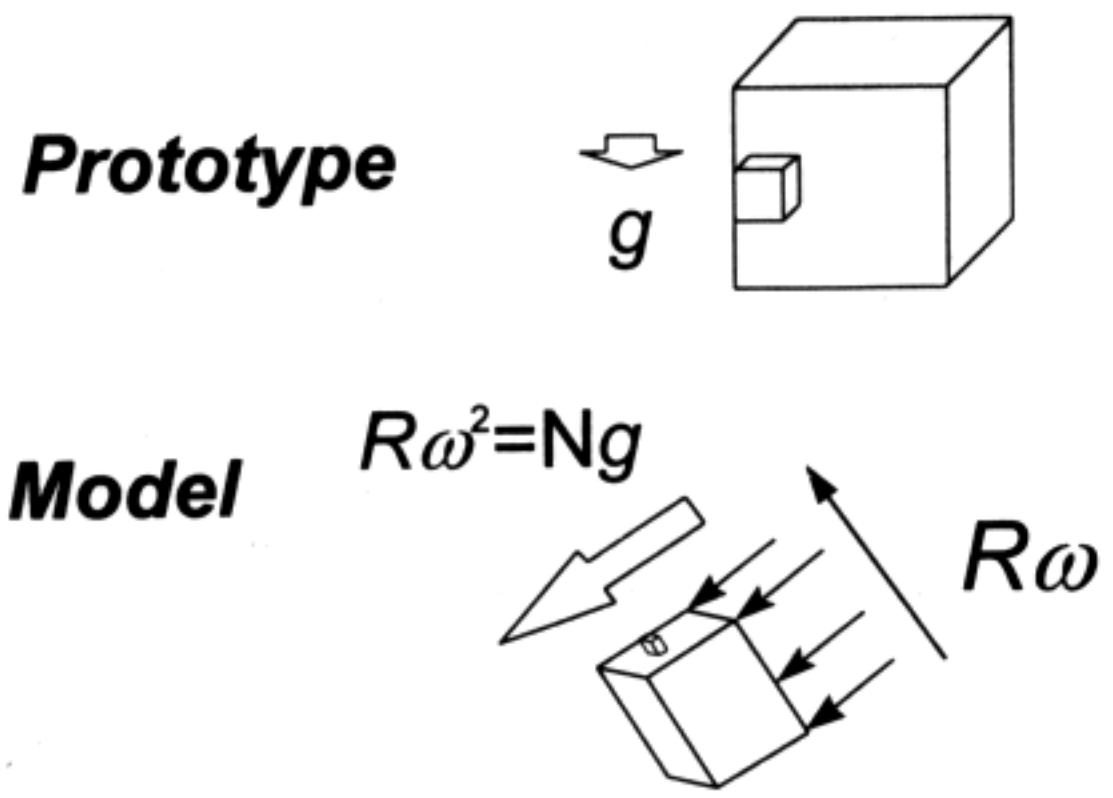

Figure 1. Effect of Acceleration on Model and Prototype, after Schofield (6).

The effect of gravitational (or any other) acceleration on capillarity is captured in the Capillary number, $Ca = \rho g H d/\sigma$. Using the same porous medium and fluids ensures that ρ, d and σ are identical in model and prototype. Moving from prototype to model, the capillary height, H, a macroscopic length, is reduced by a factor N, while the gravitational acceleration increases by N. The product gH is therefore constant. Thus, Ca in the model is identical with that in the prototype, as required for correct finger scaling.

Two length scales are important in centrifuge modelling: the particle, a microscopic, length, and the system, a macroscopic length. The minimum macroscopic length scale is an order of magnitude above the grain size. As

Table 1. Parameters and Centrifuge Scaling Criteria

Parameter and Description	Dimensions[a]	Scaling Behaviour[a]
g, magnitude of gravitational acceleration	L/T^2	N
L, macroscopic length, e.g., column length	L	1/N
d, microscopic length, e.g., particle size	L	1
w, finger width	L	1/N
V_f, finger velocity	L/T	N
U, base velocity	L/T	N
$P_c(\theta)$, capillary pressure	M/LT^2	1
$\psi(\theta)$, moisture tension	L	1/N
t, time	T	$1/N^2$
$k(\theta)$, intrinsic permeability	L^2	1
C, solute concentration	M/L^3	1
ρ, fluid density	M/L^3	1
μ, fluid viscosity	M/LT	1
θ, volumetric water content	1	1

[a]M - Mass, L - length, T - time, N - scaling factor.

mentioned, the microscopic length is invariant, because the same soil is used in model as prototype. The system lengths, however, are subject to a length reduction of N. Some examples of macroscopic lengths in subsurface hydrology are: depth of partially saturated zone, lateral extent of heterogeneities and distance between pollutant source and detection point.

Unstable wetting infiltration introduces another parameter: the perturbation wave length, or finger size. Although the product of microscopic processes that are, as yet, not clearly understood (12), unstable infiltration is manifested at a macroscopic scale. Scaling of the finger size is therefore expected to follow that of the macroscopic size, while the propagation of the finger through the soil responds as a pore velocity. Thus, relative to the prototype behaviour, the finger width in the model is expected to scale inversely with acceleration level, 1/N, while the finger velocity is expected to scale directly with acceleration level, N. Predictions of these parameters based on hydraulic properties are described in a later section.

Using the argument that the formation of unstable wetting fronts is a macroscopic phenomenon, centrifuge modelling could be a useful tool in predicting physical parameters associated with this phenomenon.
Table 2 lists the expected scaling behaviour for the critical wavelength, finger width and finger velocity. In the next section, three series of tests are discussed that examine the effect of increased acceleration on the finger spacing, size and velocity.

MODELLING GRAVITY-DRIVEN WETTING FRONT INSTABILITY

General

The set up used for investigating unstable wetting infiltration by the three series of experiments is similar in concept: the system flux is controlled by the height of water above a fine sand layer, while the transverse width of the chamber ensures the formation of two-dimensional fingers. A typical experimental apparatus is shown diagrammatically in Figure 2. A perspex window is fitted to the chamber, so that the wetting process can be followed and recorded on video tape. Two of the experimental series were conducted at the Department of Civil Engineering, University of Western Australia (13, 14), while a third series was conducted at the centrifuge facility at the Department of Civil and Environmental Engineering, Massachusetts Institute of Technology (10).

A total of 17 experiments was performed on three types of sand, and using two types of fluid. Griffioen et al. (14) used a 0.22-mm sand, while Culligan et al. (13) and Banno (10) used a sand with an average particle size of 0.6 mm. Although the 0.6-mm sands are not the same, the hydraulic properties should be similar. Results shown later, show this to be the case.

Culligan et al. (13) and Griffioen et al. (14) used water as the wetting fluid, while Banno (10) used an aliphatic oil, SOLTROL 220. The properties of the oil and water are listed in Table 3. Note that the oil density is approximately 80% that of water. This means that the oil experiments simulate LNAPL (Light Non-Aqueous Phase Liquid) infiltration. All experiments reported here, simulated a wetting fluid infiltration, the fluid being water or oil.

The observed finger spacing, width and velocity for all experiments are listed in Table 4, together with the ranges over which they varied and the test conditions for which they were observed. Next, we discuss the observed results, while further analysis is presented after the theory is discussed.

Finger Width

Results for the individual series show that the finger

Table 2. Centrifuge Scaling Relationships for Wetting Front Instability.

Finger Property	Model:Prototype Ratio
λ_c	1:N
w	1:N
V_f	N:1

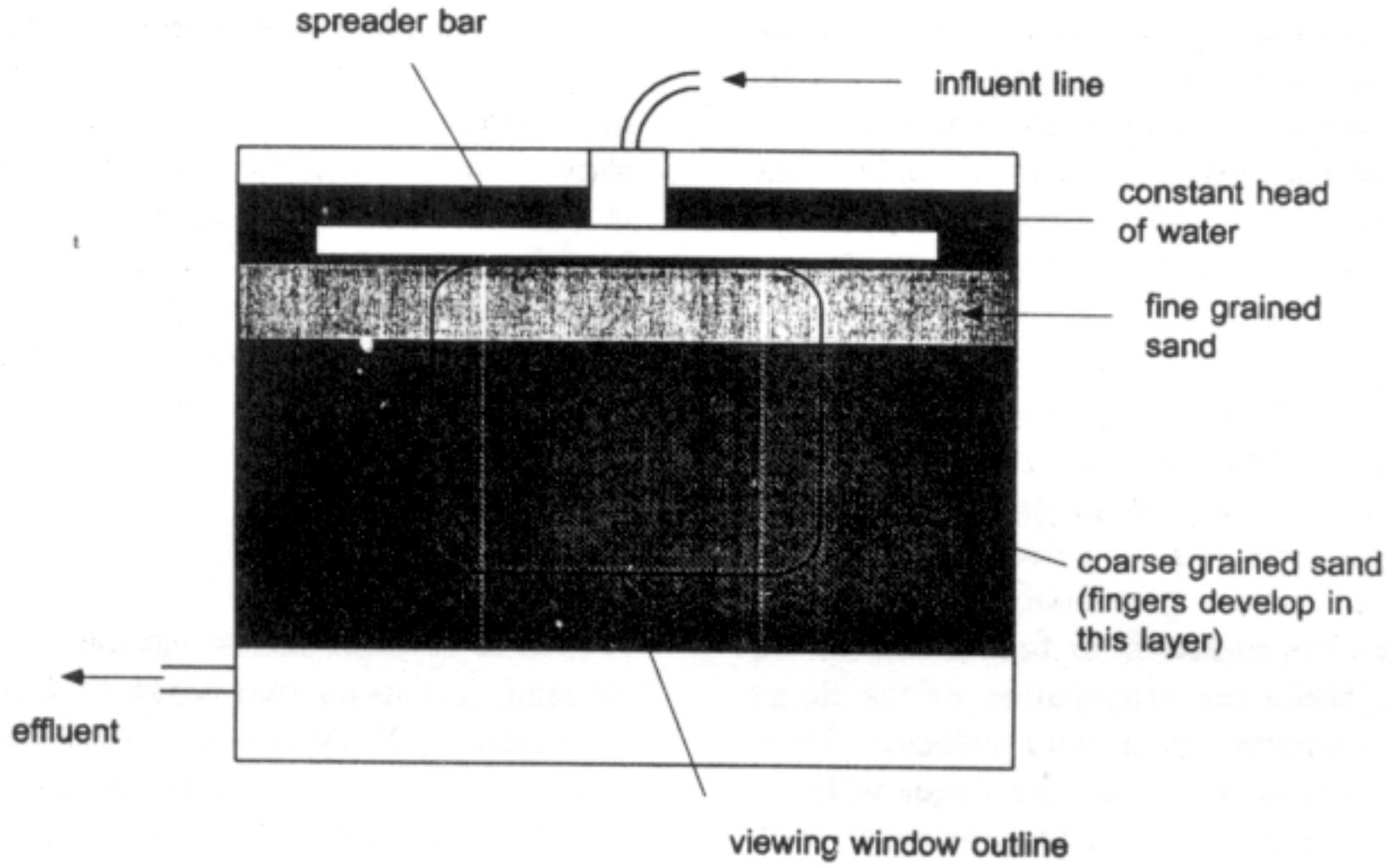

Figure 2. Typical Experimental Apparatus

Table 3. Physical Properties of SOLTROL 220 oil, and water.

	SOLTROL 220	water
dynamic viscosity (g/cm/s)	4.12×10^{-2}	8.90×10^{-3}
density (g/cm^3)	0.795	0.997
surface tension (dyne/cm)	25.3	71.9

width changes with acceleration level in accordance with the macroscopic scaling argument presented above. Figure 3 shows that the finger size for each series of experiments varies linearly with the inverse of acceleration level. Although the oil is 4 times more viscous than water, it does not produce fingers that are significantly larger than those formed by water in a similar sand: the 1*g* result of Culligan et al. (13) shows finger sizes ranging from 2 to 3 cm, while the two 1*g* experiments of Banno (10) are within a similar range.

Finger Spacing

The separation between fingers, λ, varies with acceleration level, N, as shown in Figure 4. The similarity between the results of Culligan et al. (13) and Banno (10) observed in Figure 3, is repeated in Figure 4. We also note that the slope of the trend lines are numerically similar, although there is considerable scatter in the data. The similarity between Figure 3 and Figure 4 is expected, based on the observation that unstable wetting infiltration is a macroscopic process.

The ratio of finger width to finger spacing, w/λ, represents the fraction of the cross sectional area wetted by the fingers. w/λ decreases as the acceleration level increases (Figure 5). For example, w/λ is equal to 0.73 in test 4 of Griffioen et al. (14), and steadily decreases to 0.57 at 15*g*. The common trend is for the ratio w/λ to reduce to 0.5 at higher acceleration levels. The implications of this behaviour are discussed later.

Finger Velocity

As expected from the macroscopic scaling argument, and displayed in Figure 6, the finger velocity increases

Table 4. Test Description and Observed Finger Size and Velocity

Test	fluid	acceleration level[a] (N)	finger width[b] (cm)	finger velocity[b] (cm/min)	finger spacing[b] (cm)
Culligan et al. (13)					
test 1:	water	1	2.5 ± 0.5	18 ± 3	4.75 ± 2.25
test 2:	water	10	0.25 ± 0.15	210 ± 30	0.62 ± 0.25
Griffioen et al. (14)					
test 1:	water	6.2	3.5 ± 1.5	6.5 ± 1.0	5.0 ± 1.0
test 2:	water	10	2.0 ± 0.2	9.0 ± 1.5	3.2 ± 0.2
test 3:	water	15	0.9 ± 0.2	16 ± 3	1.5 ± 0.5
test 4:	water	1.0	11.0 ± 4.0	1.0 ± 0.4	14.5 ± 2.5
Banno (10)					
test 1	oil	1.0	2.53 ± 0.82	0.90 ± 0.18	3.00 ± 0.87
test 2	oil	5.2	0.71 ± 0.17	8.22 ± 0.84	1.49 ± 0.67
test 3	oil	11	0.44 ± 0.11	14.94 ± 1.8	1.23 ± 0.37
test 4	oil	7.5	0.69 ± 0.12	9.96 ± 1.14	1.31 ± 0.44
test 5	oil	3.8	1.30 ± 0.23	4.02 ± 0.96	2.16 ± 0.90
test 6	oil	6.1	0.72 ± 0.17	6.54 ± 1.26	1.34 ± 0.38
test 7	oil	1.0	2.83 ± 1.22	0.96 ± 0.18	3.29 ± 0.99
test 8	oil	4.4	0.87 ± 0.17	4.50 ± 1.32	1.54 ± 0.71
test 9	oil	5.2	0.62 ± 0.14	5.34 ± 1.50	1.25 ± 0.35
test 10	water	1.0	3.28 ± 1.10	7.56 ± 0.60	4.68 ± 0.98

[a]The actual centrifugal acceleration is N*g*, where 1*g* is the prototype
[b]Ranges of values are included in respective figures

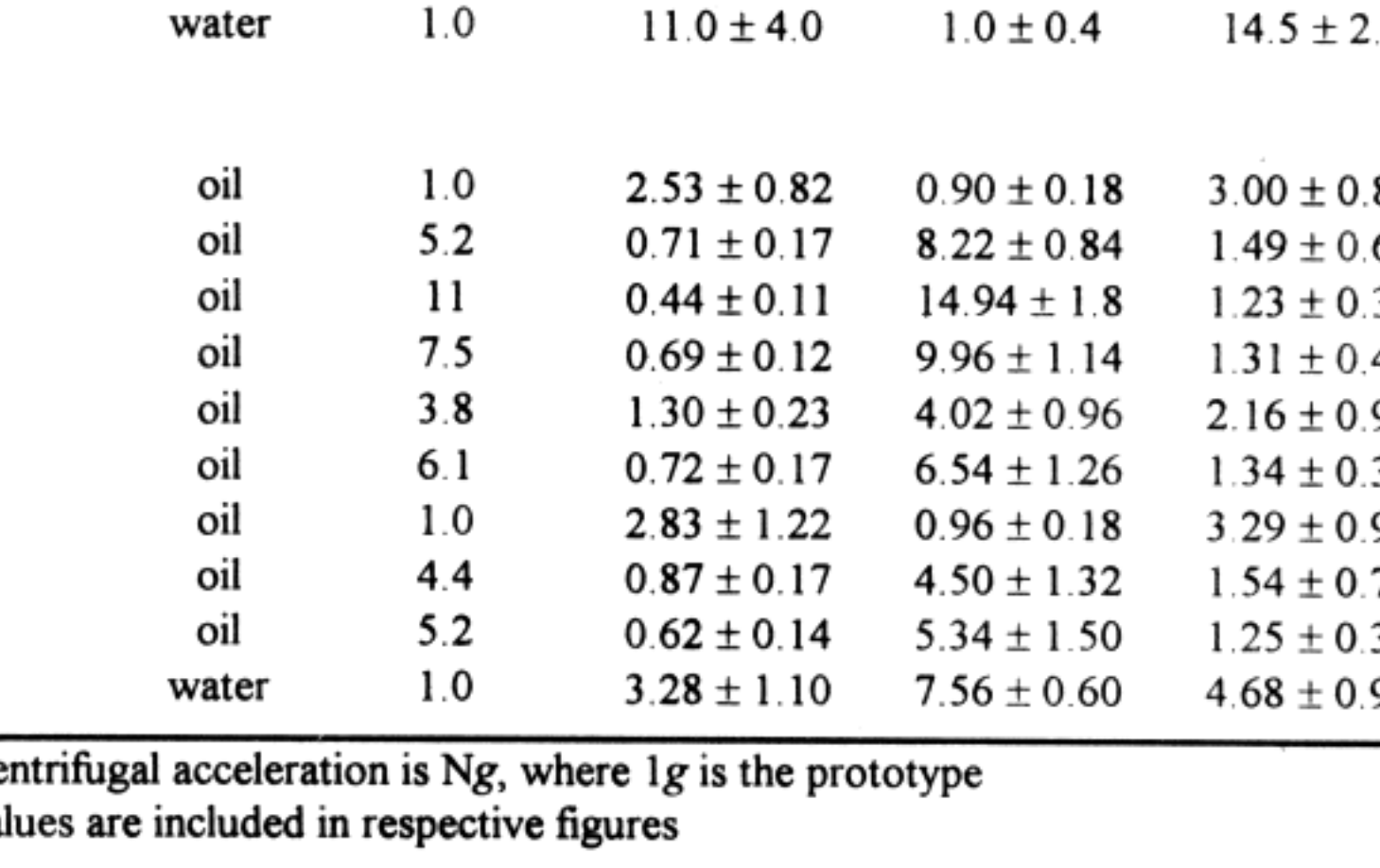

Figure 3. Variation of Finger Width, w, as Observed During Centrifuge Testing.

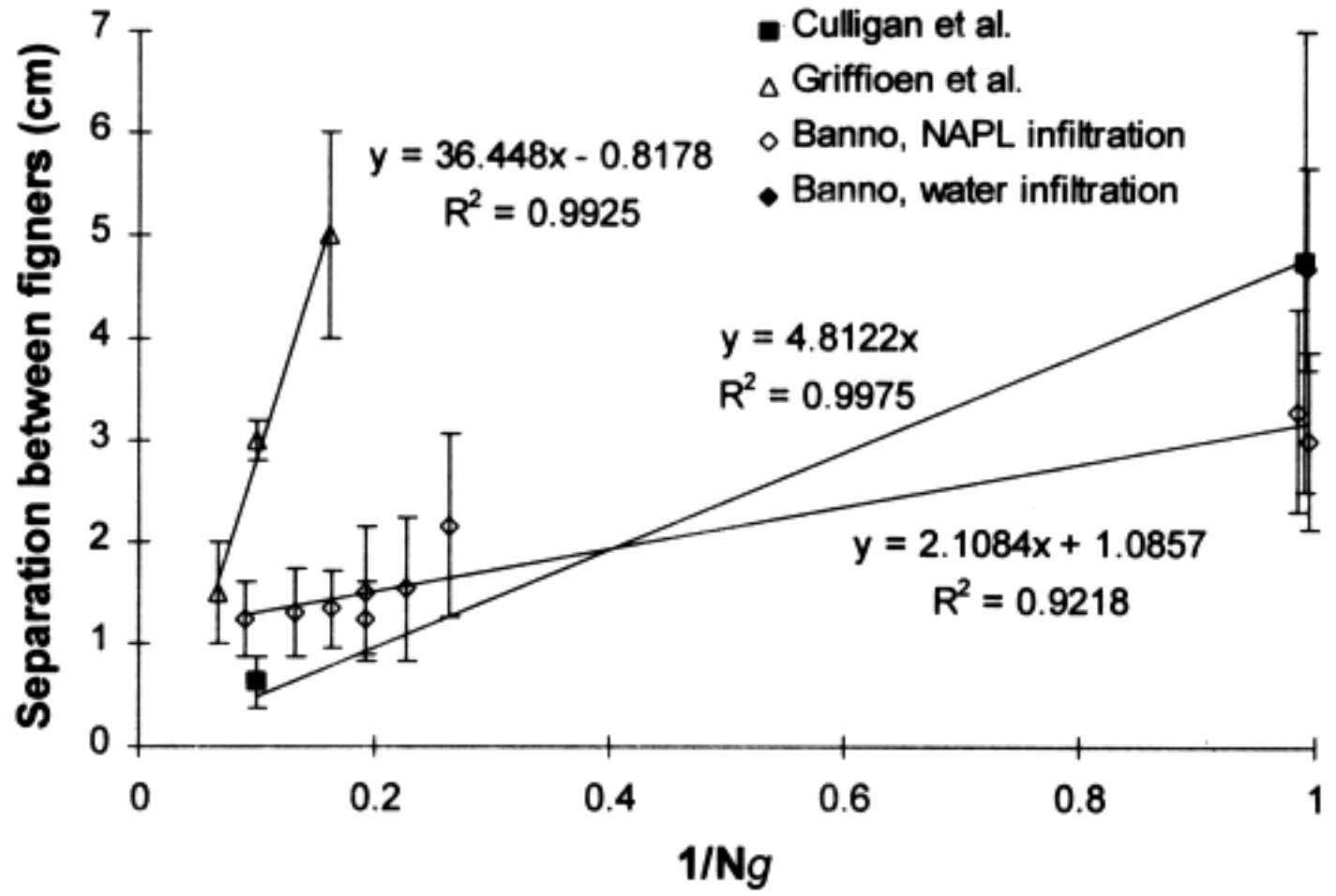

Figure 4. Spacing Between Fingers as Observed During Centrifuge Testing.

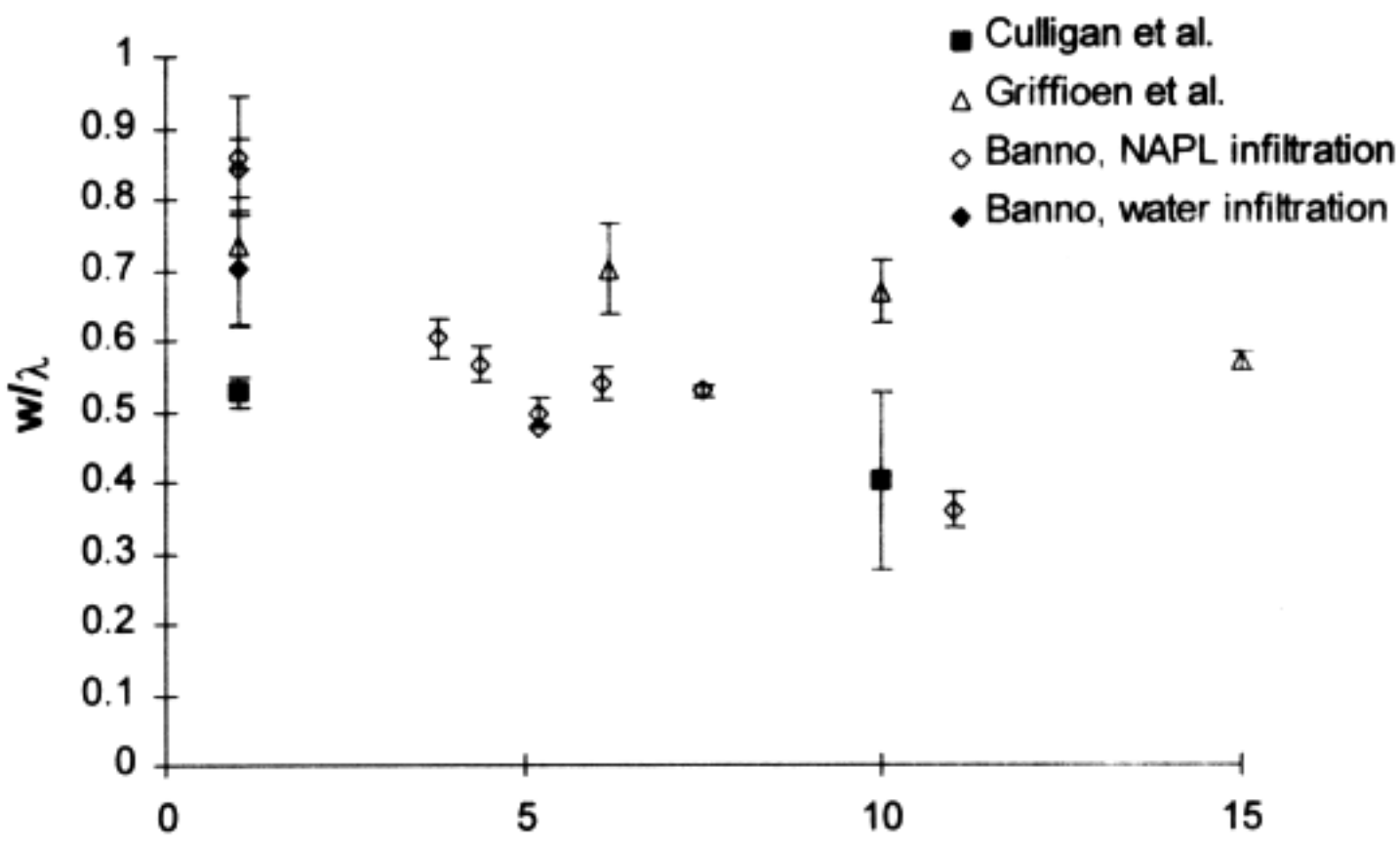

Figure 5. Ratio of Finger Width, w, to Spacing, λ, as a Function of Acceleration Level.

linearly with acceleration level. Figure 6 also shows that for a hypothetical zero gravity case, the finger velocities approach zero. At zero gravity, there is no driving force for fingering, hence velocity is also zero.

We also note the difference in velocity between two fluids in similar sands. Culligan et al. (13) used a coarse sand, and the finger velocity at 1*g* is about 18 cm/min, while the fingers in the similar sand used by Banno (10) had a propagation velocity of 0.9 cm/min at 1*g*. Density and viscosity differences obviously determine the rate of finger propagation.

Predicting Finger Width and Propagation

In two of the series (13, 14), the observed finger width was compared with those predicted from theory (presented in the next section). The hydraulic properties associated with predicting the finger width were obtained by conducting a constant-head infiltration experiment. The parameters of an infiltration formula

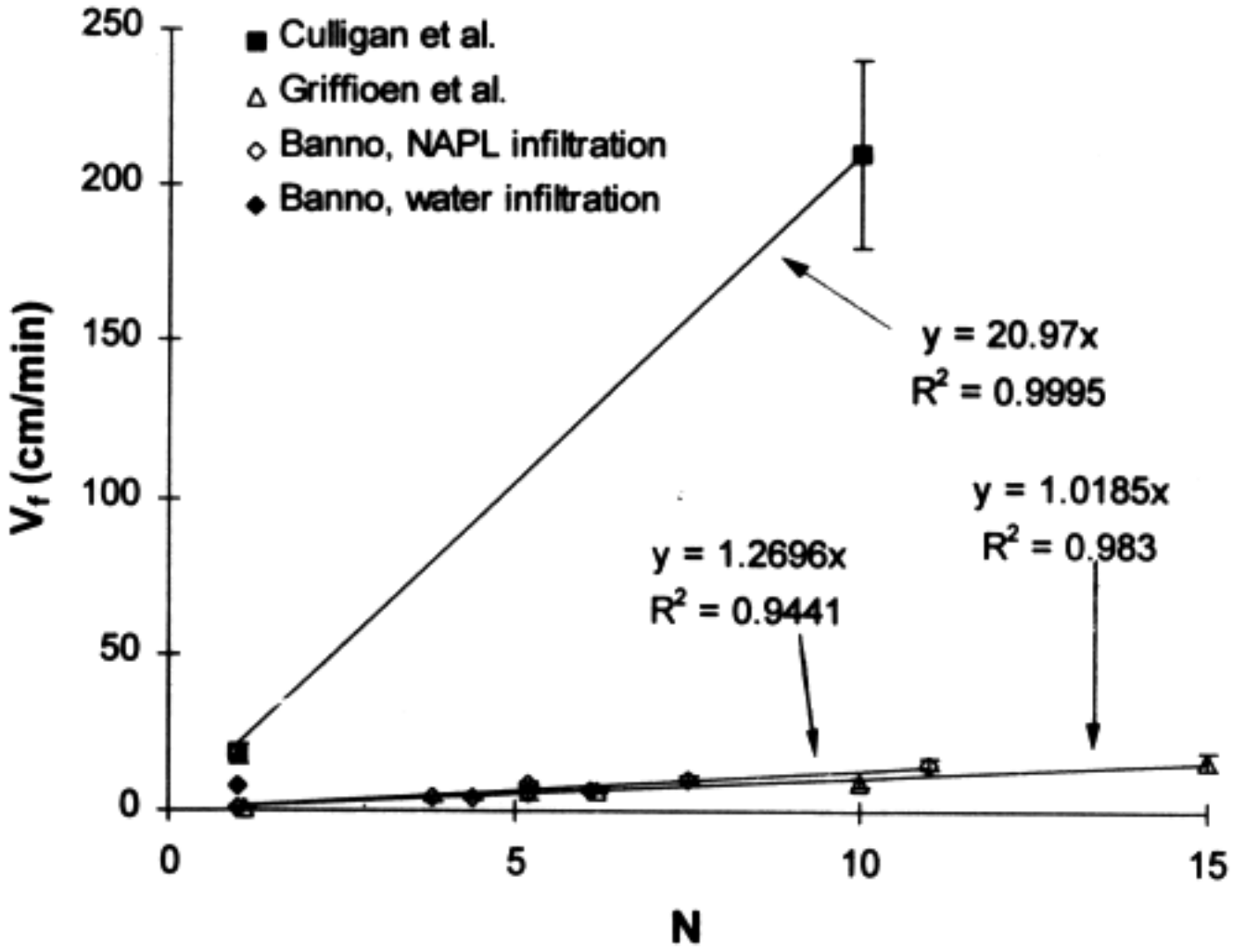

Figure 6. Variations of Finger Velocity with Acceleration.

(15) were fitted to the cumulative infiltration data. Table 5 lists the parameters obtained for the two sands. For the sand of Banno (10), the parameters were back calculated for both water and oil infiltration, and found to be in good agreement with the similar-sized sand of Culligan et al. (13).

EQUATIONS FOR UNSTABLE WETTING INFILTRATION

In order to compare the experimental results with predictions, we present, in brief, two theories for determining the onset of unstable wetting infiltration. The first, presented by Chuoke et al. (16), assumed that the pressure discontinuity at the fluid-fluid interface was proportional to the curvature of the interface. Parlange and Hill (17) assumed that the movement of the convex front increased in proportion to its curvature. Analysis and application of these theories to centrifuge testing is similar to that presented by Culligan and Barry (18).

Critical Velocity

In the absence of a porous medium, the immiscible displacement of one fluid (fluid 1) by another (fluid 2) depends on the imbalance of pressures in front of, and behind the interface. Using Darcy's law to describe fluid velocity, continuity of mass and the Laplace equation for fluid flow, the critical velocity for stability, U_c, is calculated assuming a small perturbation at the interface

Table 5. Hydraulic Properties of Soils.

Reference	wetting fluid	θ_F	K_F 10^{-2} cm/s	S^2 10^{-2} cm^2/s
Culligan et al. (13)	water	0.28	8	1
Griffioen et al. (14)	water	0.37	2.8	7.3
Banno (10)[a]	oil	0.365	0.63	0.078
	water	0.365	2.85	1.03

[a]back-calculated from observed finger behaviour

of the fluids (19),

$$U_c = \frac{(\rho_1 - \rho_2)gk}{\mu_1 - \mu_2} \quad (1)$$

For example, for downward vertical displacement of a dense, viscous fluid by a lighter, less viscous one (see Figure 7), we have $\mu_1 - \mu_2 > 0$, $\rho_1 - \rho_2 < 0$, and $U > 0$. In this configuration, viscosity is a destabilising force, while the density difference and gravity act to stabilise the front, leading to a critical velocity, U_c, above which there is instability. The four possible combinations of viscosity and density differences are shown in Table 6 for downward displacement.

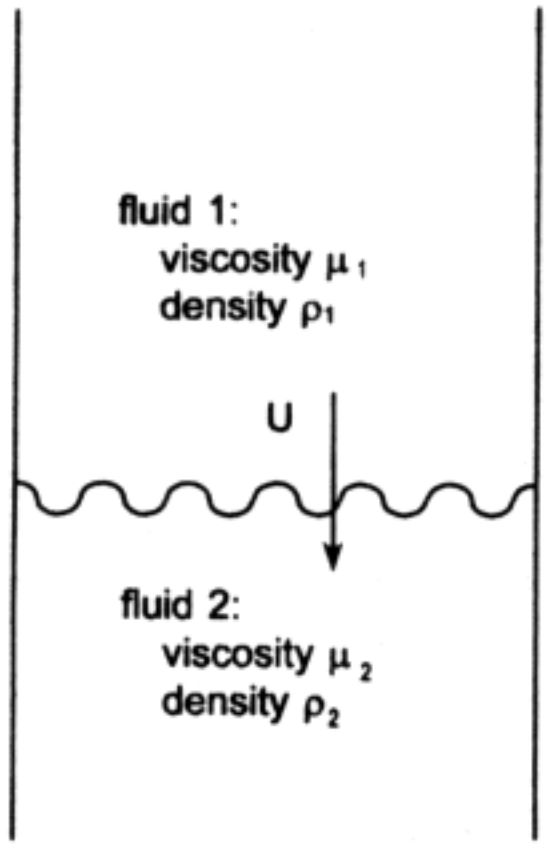

Figure 7. Immiscible Fluid Displacement

Chuoke's Theory

Surface tension effects were included by Chuoke et al. (16). Instead of predicting instability using viscosity and density alone, the curvature of the unstable front was also used. For immiscible displacements in Hele-Shaw cells, this is acceptable since the curvature of the interface is controlled by bulk fluid surface tension, a microscopic parameter. For porous media. Chuoke et al. (16) proposed an 'effective macroscopic surface tension', σ^*, which controls the curvature of the front in much the same way bulk fluid surface tension acts at the microscale. The pressure difference at the interface is therefore

$$p_1 - p_2 = \sigma^* \left[\frac{1}{r_1} + \frac{1}{r_2}\right] \quad (2)$$

Like surface tension, the macroscopic surface tension is constant but, as it is an effective parameter, it cannot be measured. Homsy (20) as well as Glass et al. (21) express doubts about the validity of Chuoke's pressure condition in porous media. Even so, it was found that estimates of finger width compared well with predictions if the macroscopic surface tension was fitted for one observed perturbation experiment (20). Equation 2 may still be used to describe the macroscopic curvature, if the macroscopic surface tension is defined as (20)

$$\sigma^* = \frac{\sigma L}{k^{1/2}} \quad (3)$$

The critical wavelength, or tip-to-tip separation, λ_c, above which the infiltration becomes unstable using Chuoke's assumption is given by

$$\lambda_c = 2\pi \left[\frac{\sigma^* k}{U\theta(\mu_2 - \mu_1) + kg(\rho_1 - \rho_2)}\right]^{1/2} \quad (4)$$

and finger width should be half the most rapidly growing wavelength (17). Thus, for an air-water system, the finger width is,

$$w = \pi \left(\frac{3\sigma^*}{\rho g} \frac{1}{1 - R_s}\right)^{1/2}, \quad (5)$$

where R_s (= q_s/K_s) is the system flux ratio.

Parlange and Hill

Instead of a pressure discontinuity at the interface, Parlange and Hill (17) assumed that the velocity across the interface is increased in proportion to its curvature. The resulting critical wavelength is (21),

$$\lambda_c = \frac{2\pi\Gamma(\mu_2 + \mu_1)\theta}{U\theta(\mu_2 - \mu_1) + kg(\rho_1 - \rho_2)}, \quad (6)$$

where Γ is defined by

$$\Gamma = \int_{\psi_o}^{\psi_f} \frac{K(\overline{\psi})d\overline{\psi}}{\theta_f - \theta_o}, \quad (7)$$

and ψ_f and θ_f are evaluated at the finger tip. Since this equation involves measurable soil properties, it is readily used. For two dimensions and specialised for an air-water system, the finger width, w, is approximated by (21, cf. 17),

$$w = \frac{\pi S^2}{K_s(\theta - \theta_o)}\left[\frac{1}{1 - R_s}\right], \quad (8)$$

Table 6. Effects of Density and Viscosity Contrast on Vertically Downward Flow.

Physical Configuration	$\rho_2 < \rho_1$	$\rho_2 > \rho_1$
$\mu_2 < \mu_1$	stable if $U < U_c$	always unstable
$\mu_2 > \mu_1$	always stable	stable if $U > U_c$

Note: fluid 2 is displacing fluid 1.

An expression for average finger velocity, V_f, has been derived using dimensional analysis at the chamber scale by Glass et al. (22)

$$V_f = \frac{K_s}{\theta_f - \theta_o} f_{vF}(R_s), \qquad (9)$$

where $f_{vF}(R_s)$ has been found by experimental work to be of the general form, (23),

$$f_{vF}(R_s) = C + R_s(1-C), \qquad (10)$$

and $C = 0.1$, at least for the experiments of Glass et al. (23).

To determine the most rapidly growing wavelength, linear stability analysis is used. However, it is worth noting that this analysis is only valid for infinitesimal disturbances. Therefore, there is no guarantee that the wavelengths which initially grow most rapidly will end up forming the dominant fingers, especially in highly non-linear systems (22). However, experiments at the laboratory scale suggest that predictions based on the theory of Parlange and Hill (17) are good, nonetheless.

APPLICATION TO CENTRIFUGE MODELLING

In order to apply centrifuge scaling arguments to these formulations of finger development, consider how the hydraulic properties of the soils behave under variations of body force. The relevant properties are hydraulic conductivity, K, sorptivity, S and moisture suction, ψ. Each of these properties is a function of the soil moisture content (the moisture content range in the case of S). Once the scaling behaviour of the hydraulic properties is established, the scaling of the finger width, spacing and velocity is presented.

Hydraulic Properties

Soil water head, ψ, is related to capillary pressure, P_c, via, $\psi = P_c/\rho g$. In this relationship, pressure and density do not change with increased acceleration. Thus, ψ reduces by a factor N during centrifugation. The moisture content associated with the range of capillary pressures, on the other hand, is independent of acceleration level. Note also that moisture suction, since it is an average behaviour over many pores, scales like a macroscopic length.

The hydraulic conductivity, K, is defined as $k\rho g/\mu$. Since viscosity, μ, density, ρ, and intrinsic permeability, k, do not change with acceleration, the hydraulic conductivity changes in the same way as the acceleration level, g.

Thirdly, the sorptivity, S, quantifies the cumulative capillary suction exerted by a soil. For example, it quantifies the rate at which water is absorbed (i.e., no gravitational flow) into a soil. For horizontal flow into a soil column, where the water is supplied to the soil at a fixed pressure head, the cumulative infiltration is $S\sqrt{t}$. Clearly, S depends on the initial moisture state of the soil and the pressure head at which the water is supplied. For unstable fingers, capillarity acts to stabilise the flow, while gravity acts to promote the instability. S depends on the moisture content of the fingers, and can be estimated from the approximate formula of Parlange (24),

$$S^2 = \int_0^{\theta_F} (\theta + \theta_F) D(\theta) d\theta, \qquad (11)$$

where we have assumed an initially dry soil. In Equation 11, $D(\theta) = K(\theta)d\psi/d\theta$, is the soil moisture diffusivity. The hydraulic conductivity, K, increases with acceleration level while the moisture suction, ψ, decreases. The sorptivity, S^2, is therefore the same in model and prototype so long as θ does not vary. Note that S^2 and Γ have a similar mathematical form. Thus,

during centrifuge modelling, they are both independent of acceleration level.

Scaling Ratios for Finger Properties

Equations 1 - 9, together with the scaling criteria of the hydraulic properties, can be used to derive scaling ratios relevant to centrifuge modelling of unstable wetting displacements.

In Chuoke's derivation (Equations 2-4), the scaling of the denominator is straightforward; density, ρ, viscosity, μ, permeability, k, and moisture content, θ, are the same in model and prototype, while base velocity, U, and gravity, g, increase by a factor N. Scaling of the effective macroscopic tension is achieved using Equation 3. The microscopic surface tension and permeability are constant, while the macroscopic length reduces by a factor N. σ^*, therefore, also reduces by the same factor. Thus, the ratio of model to prototype critical tip-to-tip separation for unstable wetting displacement is

$$\frac{\lambda_{c(m)}}{\lambda_{c(p)}} = \left[\frac{\sigma^*_{(m)}}{\sigma^*_{(p)}}\frac{(U+g)_{(p)}}{(U+g)_{(m)}}\right]^{1/2} = \left[\frac{1}{N}\frac{1}{N}\right]^{1/2} = \frac{1}{N}, \quad (12)$$

where subscripts m and p denote model and prototype, respectively.

In the same way, equation 5 and 6 from Glass et al. (22) can be scaled. The function Γ is the same in model and prototype, since it is mathematically similar to the sorptivity, S^2. At the same time, gravity and velocity increase with acceleration level in the denominator. Thus, the ratio of critical tip separation is,

$$\frac{\lambda_{c(m)}}{\lambda_{c(p)}} = \left[\frac{\Gamma_{(m)}}{\Gamma_{(p)}}\frac{(U+g)_{(p)}}{(U+g)_{(m)}}\right] = \frac{1}{N}. \quad (13)$$

Therefore, using the formulation of Glass et al. (22), the critical tip separation, or finger size, is expected to decrease by a factor N when acceleration increases by a factor N.

Finally, to ensure similitude, the scaling laws derived for flow phenomena require that the finger velocity in a centrifuge model be N times higher than those in the corresponding prototype. From Equation 8, it is clear that the finger velocity is directly related to the hydraulic conductivity, i.e,

$$\frac{V_{f(m)}}{V_{f(p)}} = \frac{K_{s(m)}}{K_{s(p)}} = N. \quad (14)$$

The finger velocity is therefore N times higher for an N-fold increase in acceleration.

DISCUSSION

The arguments for scaling of unstable wetting developed using the theory of Glass et al. (22), or that of Chuoke et al. (16), result in the same criterion as based on the assumption that unstable wetting is a macroscopic phenomenon, viz., finger width reduces by a factor N, while finger velocity increases by a factor N, for an N-fold increase in acceleration. This criterion is supported by the experimental evidence.

Finger Width According to Glass et al.

A major advantage of the Glass et al. (22) theory is the inclusion of soil hydraulic properties to predict finger width, spacing and velocity. A comparison between observed and predicted finger widths is therefore possible, if the hydraulic properties are known. Table 5 lists the results of fitting the infiltration equation of Barry et al. (15) to stable infiltration experiments for the two experiments using water as the wetting fluid.

Estimation of the finger width, relies on knowledge of the system flux ratio, R_s. Griffioen et al. (14) measured the flux and calculated the system flux ratio. For the experiments of Culligan et al. (13), R_s is estimated using the ratio of observed finger width, w, to observed finger spacing, λ_c. By conservation of mass, $wq_f = \lambda_c q_s$, where q_f is the flux in the finger and assumed equal to K_s (23), and q_s is the flux in the system. Thus, R_s (= q_s/K_s) is equal to w/λ_c. The hydraulic properties, as listed in Table 5, can then be used to calculate the expected finger widths at 1g. The 1g result for Culligan et al. (13) is predicted to be approximately 2.1 cm, which is within the range of observed finger widths (Figure 3). The average finger width for Griffioen et al. (14) is 18.4 cm, and is smaller than the value of 20 cm suggested by extrapolation (Figure 3), however, it is of the same order.

Macroscopic Surface Tension

According to the approach of Chuoke et al. (16), the macroscopic surface tension, σ^*, is constant. As shown by Culligan and Barry (18), this parameter is inversely

related to the acceleration level. The results in Figure 8, however, are inconclusive since σ^* is both constant (10) and increasing (13, 14). Use of the effective macroscopic surface tension model is therefore not recommended.

Calculating Hydraulic Properties

Estimation of the hydraulic properties for the oil-wet experiments of Banno (10) was achieved by back-calculation for the two 1*g* experiments. Hydraulic conductivity was calculated from Equations 8 and 9, assuming C = 0.2 and R_s (= w/λ_c) = 0.85, as $K_f = 6.3 \times 10^{-3}$ cm/s. Next, sorptivity was calculated to be equal to $S^2 = 1.03 \times 10^{-2}$ cm^2/s using Equation 7. These values were converted to intrinsic properties in order to calculate equivalent water-wet properties. Sorptivity was reduced to the intrinsic sorptivity, s, using the relationship $S^2 = (\sigma/\mu)s^2$ (25), while the intrinsic permeability, k, was deduced from the hydraulic conductivity. Thus, the hydraulic conductivity for both oil and water infiltration were calculated for the sand used by Banno (10). The hydraulic properties of the sand used by Banno (10) due to water infiltration and are in good agreement with the similar sand of Culligan et al. (13) (Table 5).

Viscosity and Finger Width

One result that warrants further examination is the negligible effect of viscosity on finger width in similar sands. The experiments of Culligan et al. (13) used water as the wetting fluid, while Banno (10) used a LNAPL as wetting fluid. The finger widths observed in the two series are similar. In equation 7, the finger width is a function of the hydraulic conductivity, K, defined as $k\rho g/\mu$, and the sorptivity, S^2, defined as $(\sigma/\mu)s^2$. Substituting these definitions into equation 7, leads to,

$$\mathbf{w} = \frac{\pi\sigma\mathbf{s}^2}{\mu}\frac{\mu}{\mathbf{k}\rho\mathbf{g}(\theta_\mathbf{f}-\theta_\mathbf{o})}\left[\frac{1}{1-\mathbf{R_s}}\right] = \frac{\pi\sigma\mathbf{s}^2}{\mathbf{k}\rho\mathbf{g}(\theta_\mathbf{f}-\theta_\mathbf{o})}\left[\frac{1}{1-\mathbf{R_s}}\right] \quad (15)$$

According to this equation, finger width is a function of the intrinsic soil properties (sorptivity, permeability, and change in moisture content), the fluid density, surface tension, and the imposed boundary condition, R_s. However, the viscosity, μ, does not affect finger width. Defining W^* as the ratio of finger width obtained by Culligan et al. (13) at 1*g*, to that of Banno (10), ($w_{Cull.}/w_{Banno}$), and assuming that the intrinsic soil properties and acceleration levels are the same, W^* simplifies to,

$$W^* = \frac{\sigma_{Cull.}}{\sigma_{Banno}}\frac{\rho_{Cull.}}{\rho_{Banno}}\frac{\Delta\theta_{Banno}}{\Delta\vartheta_{Cull.}}\frac{(1-R_s)_{Banno}}{(1-R_s)_{Cull.}}. \quad (16)$$

Physically, this result implies that the decrease in hydraulic conductivity that results from increasing the

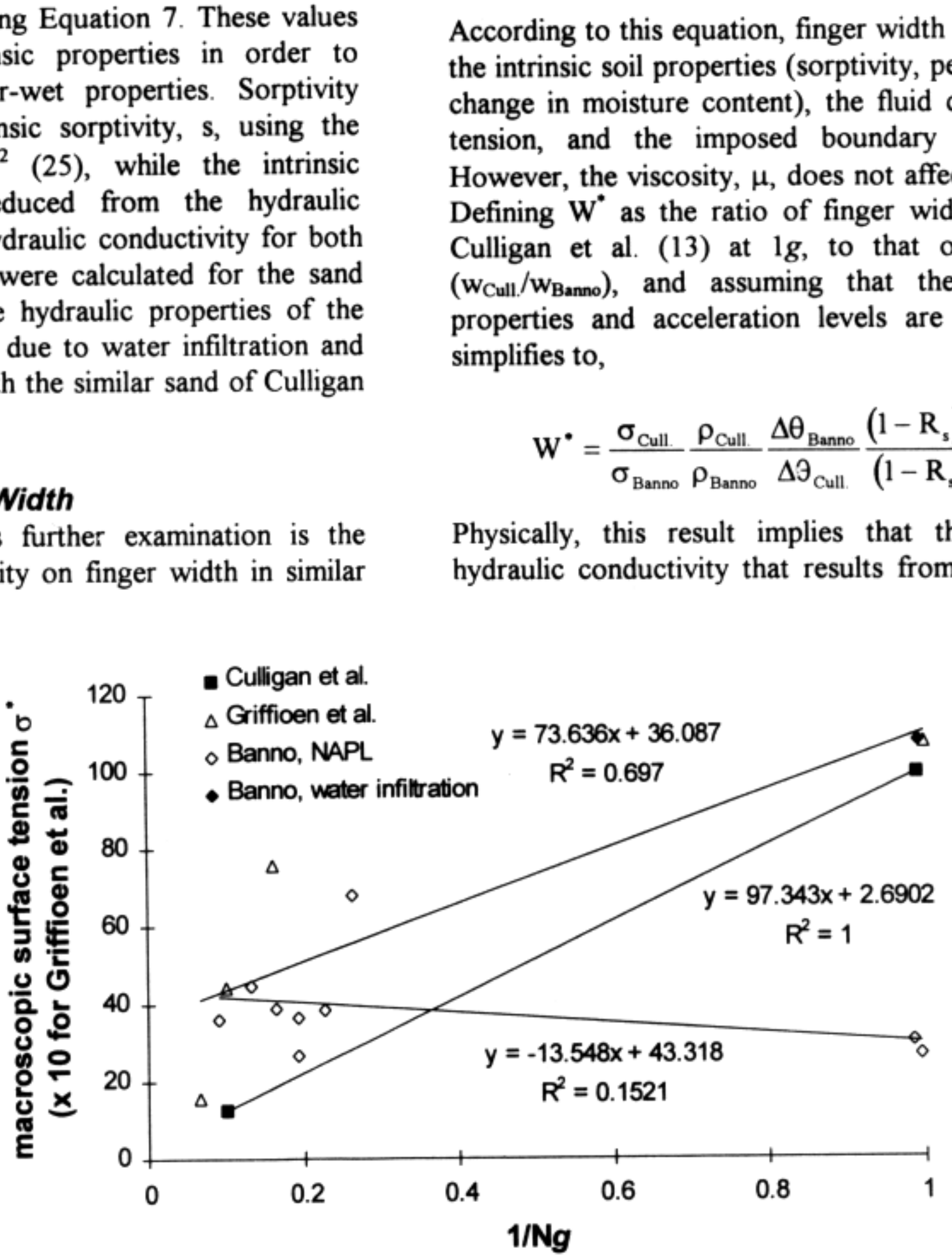

Figure 8. Macroscopic Surface Tension and Inverse of Acceleration Level

viscosity of the fingering fluid, is compensated for by a decrease in the sorptivity. Since the width of the unstable finger is a balance of a stabilising force (capillarity, or S^2) to a destabilising force (gravity, or K), changing both these factors by the same amount as a result of changing viscosity leaves the finger width unchanged. Substituting the parameters from Table 3, Table 4, and Table 5, W^* is equal to 1.03, confirming that the same size fingers are expected for the water and SOLTROL in this instance, as shown by the results in Table 4 and Figure 3.

Wetted Area Fraction, w/λ_c.

The assumption in calculating the finger width, w, is to assume that it is half the critical wavelength, λ_c (17). What has been observed in experiments (23), however, is that the fraction of soil wetted by the fingers increases as the system flux ratio increases. Thus the chamber becomes too small to observe distinct fingers as $q_s \rightarrow K_s$. In the centrifuge experiments, this effect is achieved by changing the acceleration level. At high acceleration levels, the hydraulic conductivity of the soil is increased while sorptivity and system flux ratio remain unchanged. Thus, smaller fingers are observed. As the acceleration level decreases, the finger size increases and approaches that of the chamber, until there is only one finger in which case $w/\lambda_c \sim 1$.

Finger Velocities

Although the finger widths for Culligan et al. (13) and Banno (10) are similar, we note that the propagation velocity is not. The ratio of 1*g* finger velocities observed by Culligan et al. (13) to that of Banno (10) is equal to 16.2 ± 2.3. From equation 9, it is clear that finger velocity is proportional to $K_s/\Delta\theta$. Substitution of hydraulic conductivity and change in fluid content shows that the ratio should be approximately 16. Thus, the analysis confirms the experimental results.

CONCLUSIONS

Experiments are presented which show that unstable infiltration is feasible on a geotechnical centrifuge. The tests were conducted with water or oil as the wetting fluid. Two different size sands were used. Both water and oil wetting infiltration were performed in two separate series on a similar sized sand, while water infiltration was tested in a third series on the smaller sized sand. The results of all these tests show:

(1) Finger size reduces in proportion to the applied body force, i.e., it behaves as a macroscopic length scale during centrifugal testing. At the same time, it is also a function of the average particle size, or more precisely, it varies according to S^2, where S is the sorptivity of the soil.
(2) The propagation velocity of the finger increases as a result of increased acceleration in the manner expected, i.e., in proportion to the body force.
(3) The theory of Glass et al. (23) was used successfully to show that finger width in similar soils is the same for water and SOLTROL wetting infiltration.
(4) The effective macroscopic tension, σ^*, as proposed by Chuoke et al. (16), did not perform as expected. The results of Culligan et al. (13) show that σ^* indeed varies inversely with acceleration level, while the results of Griffioen et al. (14) and Banno (10) suggest that σ^* is more or less constant.

NOTATION LIST

Ca, Capillary Number = $\rho g L d/\sigma$
d, microscopic length, e.g., particle size (L)
D, soil moisture diffusivity, (L^2/T)
g, gravitational acceleration (L/T^2)
H, capillary rise height (L)
k, intrinsic permeability (L^2)
K, hydraulic conductivity = $k\rho g/\mu$ (L/T)
L, macroscopic length, e.g., column length (L)
m, subscript to denote model
n, porosity
N, acceleration level
p, subscript to denote prototype
P_c, capillary pressure (M/LT^2)
r_1, r_2, principal radii of wetting front curvature (L)
R, centrifuge radius (L)
Re, Reynolds Number = $\rho v d/\mu$
R_f, finger flux ratio = q_f/K_s
s, intrinsic sorptivity (L^2)
S, sorptivity ($L/T^{-1/2}$)
t, time (T)
U, velocity of undisturbed front (L/T)
v, pore velocity (L/T)
V_f, finger velocity (L/T)
w, finger width (L)
W^*, ratio of finger widths
Γ, parameter incoorporating soil hydraulic properties (L^2/T)
λ_c, critical tip-to-tip separation (L)
μ, fluid viscosity (M/LT)
θ_o, θ_f, initial and finger moisture content
ρ, fluid density (M/L^3)

σ, σ^*, microscopic and macroscopic surface tension (M/T^2)
ψ, moisture tension (L)
ω, angular velocity (1/T)

REFERENCES

1. Alemi, M.H., Nielsen, D.R. & Biggar, J.W. 1976. Soil Sci. Soc. Am. J. 40, 212.
2. Cooke, A.B. & Mitchell, R.J. 1991. Can. Geotech. J. 28, 829.
3. Hensley, P.J. & Savvidou, C. 1993. Int. J. Num. Anal. Meth. Geomech. 17, 493.
4. Li, L., Barry, D.A. & Stone, K.J.L. 1994. Can. Geotech. J. 31, 471.
5. Hellawell, E.E. & Savvidou, C. 1994. In: Leung, C.F., Lee, F.H. & Tan, E.T.S. (Editors), Centrifuge 94, pg. 357, Balkema, Rotterdam.
6. Schofield, A.N. 1980. Géotechnique 30, 227.
7. Arulanandan, K., Thompson, P.Y., Kutter, B.L., Meegoda, N.J., Muraleetharan, K.K. & Yogachandran, C. 1988. J. Geotech. Eng. 144, 185.
8. Hensley, P.J. & Schofield, A.N. 1988. Géotechnique 41, 447.
9. Culligan-Hensley, P.J. & Savvidou, C. 1995. In: Taylor, R.N. (Editor) Geotechnical centrifuge technology, pg 196, Blackie Academic, London.
10. Banno, K. 1996. M. Sc., Massachusetts Institute of Technology.
11. Bear, J. and Verruijt, A. 1987. Modelling groundwater flow and pollution, Reidel Publishing Company.
12. Glass, R.J. & Nicholl, M.J. 1996. Geoderma 70, 133.
13. Culligan, P.J., Barry, D.A. & Parlange, J.-Y. 1996. Can. Geotech. J. (submitted).
14. Griffioen, J.W., Barry, D.A. & Culligan, P.J. 1996. manuscript in preparation.
15. Barry, D.A., Parlange, J.-Y., Haverkamp, R. & Ross, P.J. 1995. Soil Sci. 160, 8.
16. Chuoke, R.L., van Meurs, P. & van der Poel, C. 1959. Petrol. Trans. AIME 216, 188.
17. Parlange, J.-Y. & Hill, D.E. 1976. Soil Sci. 122, 236.
18. Culligan, P.J. & Barry, D.A. 1996. Report WP1207PC, Dept. Env. Eng., Univ. West. Aust.
19. Hill, S. 1952. Chem. Eng. Sci. 1, 247.
20. Homsy, G.M. 1987. Ann. Rev. Fluid Mech. 19, 271.
21. Glass, R.J., Parlange, J.-Y. & Steenhuis, T.S. 1991. Water Resour. Res. 27, 1947.
22. Glass, R.J., Parlange, J.-Y. & Steenhuis, T.S. 1989a. Water Resour. Res. 25, 1187.
23. Glass, R.J., Parlange, J.-Y. & Steenhuis, T.S. 1989b. Water Resour. Res. 25, 1195.
24. Parlange, J.-Y. 1975. Soil Sci. Soc. Am. Proc. 39, 415.
25. Philip, J.R. 1957. Soil Sci. 84, 257.